Journal of Applied Mechanics and Technical Physics, Vol. 43, No. 5, pp. 710–717, 2002

HEAT TRANSFER ON THE SURFACE ON A SPHERICALLY BLUNTED CONE EXPOSED TO A SUPERSONIC SPATIAL FLOW WITH INJECTION OF A COOLANT GAS

V. I. Zinchenko and A. Ya. Kuzin

UDC 536.24.01

The heat-transfer processes in a supersonic spatial flow around a spherically blunted cone with allowance for heat overflow along the longitudinal and circumferential coordinates and injection of a coolant gas are studied numerically. The prospects of using highly heat-conducting materials and injection of a coolant gas for reduction of the maximum temperatures at the body surface are demonstrated. The solutions of the direct and inverse problems in one-, two-, and three-dimensional formulations for different shell materials are compared. The error of the thin-wall method in determining the heat flux on the heat-loaded boundary of the body is estimated.

One of the most complicated problems in interaction of high-enthalpy gas flows with flying vehicles is the thermal protection of the constructions of the latter. Both active and passive methods of thermal protection are used in practice, as well as the combined method: injection of a coolant gas into a high-enthalpy gas flow from porous elements of constructions, combined with heat overflow on the surface caused by a proper choice of the highly heat-conducting material of the composite shell [1–6]. The study of heat transfer under these conditions is performed by solving direct [1–3] and inverse [4–6] problems. Methods of solving inverse problems (IP) are particularly important because of the lack of information on the processes under study and increase requirements to the accuracy of determining the heat-transfer characteristics of the body shell with allowance for the fact that the heat- and mass-transfer processes are nonlinear, multidimensional, and multiparametric [7].

An effective method of solving multidimensional boundary-value IP is the method of iterative regularization proposed in [8] and developed in other papers. Based on this method, Alifanov and Nenarokomov [9, 10] developed algorithmic and program software for the experimental-numerical method of diagnostics f the external thermal action on multilayered elements of constructions, where the heat transfer is described by a three-dimensional heat-conduction equation in various coordinate systems. The method of iterative regularization in complex mathematical models is complemented by regularization numerical methods [4–6, 11]. The necessity of using three-dimensional formulations of IP for supersonic spatial flow analysis is caused by the fact that, in the case of motion of a flying vehicle at incidence, heat overflow occurs not only along the longitudinal but also along the circumferential coordinate due to the large difference in heat fluxes on the leeward and windward sides [6]. Injection of a coolant gas decreases the temperature in the region of the porous spherical bluntness and favors heat overflow from the peripheral part of the cone to the porous nose [3, 4]. However, there is no detailed study of the influence of injection on the reconstructed temperature and heat flux in a wide range of thermophysical characteristics of the shell material in the case of a spatial flow around the body in the literature. It is also of interest to estimate the limits of applicability of one- and two-dimensional approaches and the thin-wall method for determining heat fluxes at the body boundary.

The effect of heat overflow and injection of a coolant gas on heat-transfer characteristics in a wide range of thermophysical parameters of the shell material is considered in the present work using the full mathematical formulation of the problem of heating a spherically blunted cone with allowance for injection of a coolant gas from the porous spherical part in a supersonic spatial flow and the algorithms developed for solving direct and inverse

Institute of Applied Mathematics and Mechanics, Tomsk State University, Tomsk 634050. Translated from Prikladnaya Mekhanika i Tekhnicheskaya Fizika, Vol. 43, No. 5, pp. 87–96, September–October, 2002. Original article submitted December 3, 2001; revision submitted March 19, 2002.

 0021-8944/02/4305-0710 $27.00

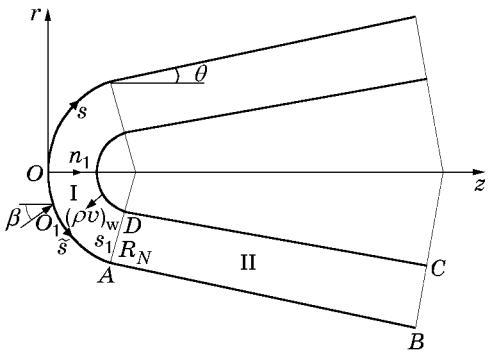

Fig. 1

three-dimensional heat-transfer problems [6]. The possibility of using one-, two-, and three-dimensional algorithms for solving direct and inverse heat-transfer problems and the thin-wall method for reconstructing the heat fluxes and temperature on the body surface is analyzed.

1. Physical and Mathematical Formulation of Direct and Inverse Problems. Heating of a spherically blunted cone exposed to a supersonic air flow at incidence is considered (Fig. 1). The shell consists of a permeable spherical and impermeable conical parts. The process of filtration of the injected gas in the direction normal to the surface is one-dimensional, and the temperature of the porous medium is uniform. The problem is considered in the natural coordinate system with the origin at the point of intersection of the axis of symmetry of the body with the surface. We write the equation of conservation of energy for the porous spherical bluntness (region I in Fig. 1)

$$c_\Sigma \frac{\partial T_1}{\partial t} - c_{p,\mathrm{g}} \frac{(\rho v)_\mathrm{w} r_{1\mathrm{w}}}{H r_1} \frac{\partial T_1}{\partial n_1}$$

$$= \frac{1}{H r_1}\Big[\frac{\partial}{\partial n_1}\Big(H r_1 \lambda_\Sigma \frac{\partial T_1}{\partial n_1}\Big) + \frac{\partial}{\partial s}\Big(\frac{r_1 \lambda_\Sigma}{H}\frac{\partial T_1}{\partial s}\Big) + \frac{\partial}{\partial \eta}\Big(\frac{H}{r_1}\lambda_\Sigma \frac{\partial T_1}{\partial \eta}\Big)\Big] \qquad (0 < s < s_A) \tag{1.1}$$

and the equation of heat conduction for the conical part of the shell (region II in Fig. 1)

$$(r\rho c_p)_2 \frac{\partial T_2}{\partial t} = \frac{\partial}{\partial n_1}\Big(r_2 \lambda_2 \frac{\partial T_2}{\partial n_1}\Big) + \frac{\partial}{\partial s}\Big(r_2 \lambda_2 \frac{\partial T_2}{\partial s}\Big) + \frac{1}{r_2}\frac{\partial}{\partial \eta}\Big(\lambda_2 \frac{\partial T_2}{\partial \eta}\Big)$$

$$(s_A < s < s_B, \qquad 0 < n_1 < L, \qquad 0 < \eta < \pi, \qquad 0 < t \leqslant t_\mathrm{fin}). \tag{1.2}$$

The initial and boundary conditions are

$$T_i|_{t=0} = T_\mathrm{in}, \qquad i = 1, 2; \tag{1.3}$$

$$q_\mathrm{w} - \varepsilon_1 \sigma T_{1\mathrm{w}}^4 = -\lambda_\Sigma \frac{\partial T_1}{\partial n_1}\Big|_\mathrm{w}, \quad 0 \leqslant s < s_A, \quad q_\mathrm{w} - \varepsilon_2 \sigma T_{2\mathrm{w}}^4 = -\lambda_2 \frac{\partial T_2}{\partial n_1}\Big|_\mathrm{w}, \quad s_A \leqslant s \leqslant s_B; \tag{1.4}$$

$$\lambda_\Sigma \frac{\partial T_1}{\partial n_1}|_L = \frac{r_{1\mathrm{w}} c_{p,\mathrm{g}} (\rho v)_\mathrm{w}}{(H r_1)_L}\,(T_\mathrm{in} - T\Big|_L), \qquad 0 \leqslant s < s_D; \tag{1.5}$$

$$\frac{\partial T_2}{\partial n_1}\Big|_L = 0, \qquad s_D \leqslant s \leqslant s_C; \tag{1.6}$$

on the junction circle AD,

$$\frac{\lambda_\Sigma}{H}\frac{\partial T_1}{\partial s} = \lambda_2 \frac{\partial T_2}{\partial s}, \qquad T_1 = T_2, \tag{1.7}$$

on the line BC,

$$\frac{\partial T_2}{\partial s} = 0, \tag{1.8}$$

and in the plane of symmetry,

$$\frac{\partial T_i}{\partial \eta}\Big|_{\eta=0} = \frac{\partial T_i}{\partial \eta}\Big|_{\eta=\pi} = 0, \qquad i = 1, 2; \tag{1.9}$$

$$H = (R_N - n_1)/R_N, \qquad r_1 = (R_N - n_1)\sin\bar{s}, \qquad r_2 = (R_N - n_1)\cos\theta + (s - s_A)\sin\theta,$$

$$\bar{s} = s/R_N, \qquad s = s_A + \cos^{-1}\theta[z + (\sin\theta - 1)R_N].$$

In (1.1)–(1.9), t is the time, r and z are the transverse and longitudinal components of the cylindrical coordinate system, n_1, s, and η are the components of the natural coordinate system, T is the temperature, ρ is the true density, $(\rho v)_{\rm w}$ is the flow rate of the coolant gas, c_p and λ are the heat capacity and thermal conductivity, H, r_1, and r_2 are the Lamé coefficients, R_N is the radius of spherical bluntness, σ is the Stefan–Boltzmann constant, ε_i $(i = 1, 2)$ is the emissivity of the surface of the wetted material, $q_{\rm w}$ is the convective heat flux from the gas phase, θ is the angle of conicity, and L is the shell thickness. The subscript "w" refers to conditions at the interface of gaseous and solid phases, "g" to the characteristics of the gas in the porous medium, "in" and "fin" to the initial and final parameters, respectively, subscripts 1 and 2 refer to regions I and II of the composite shell, respectively; the quantities at the internal surface of the shell and total values of the parameters are denoted by subscripts L and Σ, respectively; the dimensionless quantities are denoted by bar.

In solving the direct problem (DP) of determining the temperature $T(n_1, s, \eta, t)$ in the composite shell, the heat flux from the gas phase $q_{\rm w}$ is set by formulas from [12] for the case of spatial (laminar or turbulent) boundary-layer flow. Attenuation of the heat flux due to injection of the coolant gas whose composition coincides with the incoming air flow is taken into account by formulas from [13]. As a result, in a coordinate system fitted to the stagnation point O_1, we obtain the following relations on the porous spherical part of the shell: for the laminar boundary-layer flow,

$$q_{\rm w} = (\alpha/c_p)^0[1 - 0.6(\rho v)_{\rm w}/(\alpha/c_p)^0](h_r - h_{\rm w}); \tag{1.10}$$

$$(\alpha/c_p)^0 = 1.05V_\infty^{1.08}[0.55 + 0.45\cos(2\tilde{s})]/(R_N/\rho_\infty)^{0.5}; \tag{1.11}$$

$$h_r = h_{e0}[(p_e/p_{e0})^{(\gamma-1)/\gamma} + (u_e/v_m)^2 {\rm Pr}^{\,0.5}], \qquad 0 \leqslant \tilde{s} \leqslant \tilde{s}_*; \tag{1.12}$$

for the turbulent flow regime,

$$q_{\rm w} = (\alpha/c_p)^0 \exp[-0.37(\rho v)_{\rm w}/(\alpha/c_p)^0](h_r - h_{\rm w}); \tag{1.13}$$

$$(\alpha/c_p)^0 = 16.4V_\infty^{1.25}\rho_\infty^{0.8}(3.75\sin\tilde{s} - 3.5\sin^2\tilde{s})/[R_N^{0.2}(1 + h_{\rm w}/h_{e0})^{2/3}]; \tag{1.14}$$

$$h_r = h_{e0}[(p_e/p_{e0})^{(\gamma-1)/\gamma} + (u_e/v_m)^2 {\rm Pr}^{\,1/3}], \qquad \tilde{s}_* < \tilde{s} < \tilde{s}_1; \tag{1.15}$$

$$u_e/v_m = [1 - (p_e/p_{e0})^{(\gamma-1)/\gamma}]^{0.5}, \quad h_{e0} = h_\infty[1 + 0.5(\gamma - 1){\rm M}_\infty^2], \quad h_{\rm w} = b_1 T_{\rm w} + b_2 T_{\rm w}^2/2,$$

$$\tilde{s} = \arccos(\cos\bar{s}\cos\beta + \sin\bar{s}\sin\beta\cos\eta), \qquad v_m = (2h_{e0})^{0.5}.$$

To estimate the effect of injection on the heat flux in the screening zone, we use the data of [14] and formulas of [2] obtained on the basis of processing the results of numerical calculations of a spatial turbulent boundary layer and viscous shock layer [15, 16]:

$$q_{\rm w} = \left(\frac{\alpha}{c_p}\right)^0 (1 - \zeta_1 b^{\zeta_2})(h_r - h_{\rm w}), \qquad \left(\frac{\alpha}{c_p}\right)^0 = \frac{16.4V_\infty^{1.25}\rho_\infty^{0.8}2.2(p_e/p_{e0})(u_e/v_m)}{R_N^{0.2}(1 + h_{\rm w}/h_{e0})^{2/3}k^{0.4}\bar{r}_{2{\rm w}}^{0.2}},$$
$$k = (\gamma - 1 + 2/{\rm M}_\infty^2)/(\gamma + 1), \qquad \tilde{s}_A \leqslant \tilde{s} \leqslant \tilde{s}_B. \tag{1.16}$$

For the law of injection of the coolant gas $(\rho v)_{\rm w}(\tilde{s}) = (\rho v)_{\rm w}(0)(1 + a\sin^2\tilde{s})$, the following relation is valid [2]:

$$b = \frac{2(\rho v)_{\rm w}(0)\{1 - \cos\tilde{s}_1 + a[2/3 - \cos\tilde{s}_1 + (1/3)\cos^3\tilde{s}_1]\}}{(\alpha/c_p)^0(\bar{s} - \bar{s}_1)[2\cos\theta + (\bar{s} - \bar{s}_1)\sin\theta]},$$

$$\cos\tilde{s}_1 = \cos\bar{s}_1\cos\beta + \sin\bar{s}_1\sin\beta\cos\eta, \qquad \bar{s}_1 = \bar{s}_A = \pi/2 - \theta.$$

In (1.10)–(1.16), p is the pressure, h is the enthalpy, α is the heat-transfer coefficient, $\tilde{s}_*$ is the coordinate of the laminar–turbulent transition point in the coordinate system with the origin at the stagnation point, ζ_1 and ζ_2 are parameters of approximation, β is the angle of attack, Pr is the Prandtl number, V_∞, ρ_∞, and ${\rm M}_\infty$ are the free-stream velocity, density, and Mach number, and γ is the ratio of specific heats. The subscript $e0$ corresponds to conditions at the outer edge of the boundary layer and the subscript ∞ refers to free-stream conditions; the

characteristic parameters are denoted by the asterisk; the superscript 0 indicates the heat-transfer parameters α/c_p and $q_{\rm w}$ in the absence of injection.

In solving the three-dimensional IP, the temperature $T_{\rm w}(s,\eta,t)$ and convective $[q_{\rm w}(s,\eta,t)]$ and total $[Q_{\rm w}(s,\eta,t) = q_{\rm w}(s,\eta,t) - \varepsilon\sigma T_{\rm w}^4]$ heat fluxes at the boundary are determined by the mathematical model (1.1)–(1.3), (1.5)–(1.9) with an additional condition: definition of the temperature on the back surface of the shell as a function of the longitudinal and circumferential coordinates and time $T(L,s,\eta,t) = T_L^{\rm exp}(s,\eta,t)$.

2. Algorithms of Solving Direct and Inverse Problems. In solving three-dimensional DP and IP, we used algorithms of [6] based on the method of splitting in terms of spatial variables n_1, s, and η [17]. In the DP, one-dimensional equations of conservation of energy and heat conduction, which were obtained by splitting at each time layer, in the n_1, s, and η directions were calculated with a variable step by the iterative–interpolation method (IIM) [18]. The special feature of temperature calculation in the s direction was the fact that it was a continuous calculation beginning from the windward side with the condition of equal temperatures and heat fluxes ("matching" condition) at the point $s = 0$, since the condition of symmetry is invalid at this point if the body moves at incidence. As a result, the circumferential coordinate η varied within the range $[0, \pi/2]$, and the temperature for other values of η was determined from the condition of symmetry at the points $\eta = 0$ and $\eta = \pi$. In calculating temperature in all directions, we used a system of difference equations with a tridiagonal matrix, which was obtained using the logical scheme of the IIM for a parabolic generic equation with extremely general boundary conditions, including conditions of the first, second, and third kind [18]. The systems of difference equations were solved by the method of nonmonotonic sweep in the directions n_1 and s and by the method of cyclic sweep [19] with iterations over coefficients with a given accuracy in the direction η.

After application of the method of splitting in terms of spatial variables, the IP was solved in three stages at each time layer. At the first stage, the temperature in the direction n_1 was calculated on the basis of a specific temperature $T_L^{\rm exp}(s,\eta,t)$ by the method used in [6], where the difference scheme was obtained for a parabolic generic equation and allows one to take into account the injection of the coolant gas. Using this temperature at the initial condition, the temperature in the direction s was determined at the second stage by the IIM. The temperature in the direction η was found at the third stage in a similar manner. Then we passed to the next time layer and repeated the procedure. Based on the resultant temperature field, we determined the total heat flux $Q_{\rm w}(s,\eta,t)$, and, then, form the boundary conditions (1.4), the convective heat flux $q_{\rm w}(s,\eta,t)$.

This method of solving the three-dimensional IP allows one to study both fast and slow heat-transfer processes. The stability of the solution is achieved by using the IIM implicit difference scheme related to the spline theory [20] and by smoothing the initial temperature $T_L^{\rm exp}(s,\eta,t)$ by methods from [21, 22] or by solution regularization by Tikhonov's method [8]. A stable solution is also obtained by using one- and two-dimensional cubic B-splines [23] for data approximation. The above methods of suppressing instability of the solution are used in solving various one-dimensional [11] and also two- and three-dimensional [4–6] inverse problems.

3. Results of Numerical Calculations. Three-dimensional DP and IP were solved numerically using programs developed in the Fortran code. The time of solving the three-dimensional reference variants of DP and IP up to a steady temperature distribution ($t = 200$ sec) on a $11 \times 41 \times 13$ computational grid was approximately 9 min on a Pentium-3 computer. The direct and inverse spatial problems were tested both at the level of individual program modules and at the level of programs as a whole. The basic program modules, such as the solution of the one-dimensional parabolic generic equation with the extremely general boundary conditions and the solution of the one-dimensional boundary-value IP for this case, were compared with the known solutions [18, 24]. The spatial DP in the particular case $t \to \infty$ without allowance for heat overflow in the directions s and η was tested by comparing the steady temperature of the surface with the radiative equilibrium temperature $T_{\rm w,eq}$. In solving the DP in the full formulation, the steady temperature of the surface satisfied the relation [3]

$$\int\limits_0^{\pi} \left\{ \int\limits_0^{s_A} r_{1\rm w}[q_{\rm w} - \varepsilon_1\sigma T_{\rm w}^4 + c_{p,\rm g}(\rho v)_{\rm w}(T_{\rm in} - T_{\rm w})]\, ds + \int\limits_{s_A}^{s_B} r_{2\rm w}(q_{\rm w} - \varepsilon_2\sigma T_{\rm w}^4)\, ds \right\} d\eta = 0,$$

which is obtained by integrating the initial boundary-value problem (1.1)–(1.9) in the steady case. The numerical solutions of [3, 6] were also used as tests. The spatial IP was tested by comparison with the "exact" solution, which was assumed to be the numerical solution of the spatial DP.

The boundary-layer flow on the porous spherical shell was assumed to be laminar in the vicinity of the stagnation point and turbulent on the remaining part of the spherical shell and on the cone. We used a widely used

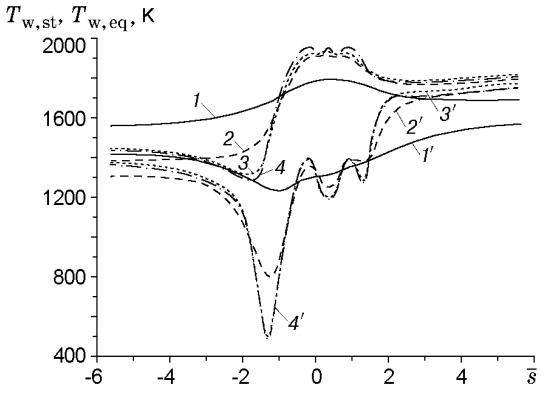

Fig. 2

model of point transition from the laminar to the turbulent flow regime. The transition point $\tilde{s}_*$ was determine from the condition of the change of the sign of the difference in the values of α/c_p for the laminar (1.11) and turbulent (1.14) flow regimes in the region $[0, \tilde{s}_1]$, and the position of this point depended on the parameters in Eqs. (1.11) and (1.14).

The calculations were performed for the following values of the governing parameters borrowed from [3, 6]: $c_\Sigma = c_{p1}\rho_1(1-\varphi) + c_{p,g}\rho_g\varphi$, $\lambda_\Sigma = \lambda_1(1-\varphi) + \lambda_g\varphi$, $c_{p,g} = b_1 + b_2T$, $b_1 = 965.5$, $b_2 = 0.147$, $T_{in} = T_\infty = 300$ K, $c_{p\infty} = 10^3$ J/(kg·K), $\rho_g = 1.3$ kg/m^3, $\lambda_g = 0.026$ W/(m·K), $L = 0.005$ m, $\varepsilon_i = 0.85$ $(i = 1, 2)$, $R_N = 0.0185$ m, $\rho_\infty = 0.208$ kg/m^3, $V_\infty = 2080$ m/sec, $\beta = 20°$, $\theta = 5°$, porosity $\varphi = 0.34$, $\gamma = 1.4$, $M_\infty = 6$, Pr $= 0.72$, $\zeta_1 = 0.285$, $\zeta_2 = 0.165$, and $a = 0$. As in [6], we considered shell materials with a wide range of thermophysical characteristics: copper [$\lambda = 386$ W/(m·K), $\rho = 8950$ kg/m^3, and $c_p = 376$ J/(kg·K)], coal–plastic [$\lambda = 0.75$ W/(m·K), $\rho = 1350$ kg/m^3, and $c_p = 1062$ J/(kg·K)), and steel [$\lambda = 20$ W/(m·K), $\rho = 7800$ kg/m^3, and $c_p = 600$ J/(kg·K)]. The pressure distribution on the body surface p_e/p_{e0} was found by solving the spatial gas-dynamic problem [25].

Figures 2–4 and 5–6 show the solutions of direct and inverse heat-transfer problems, respectively, in the planes of symmetry $\eta = 0$ and $\eta = \pi$.

Figure 2 shows the influence of injection of the coolant gas on the distribution of the steady temperature $T_{w,st}$ over the surface ($t = 200$ sec) (curves 1–3 and 1′–3′) and the radiative equilibrium temperature $T_{w,eq}$ (curves 4 and 4′) on the windward ($\bar{s} > \bar{s}_{O_1}$) and leeward ($\bar{s} \leqslant 0 \cup 0 < \bar{s} < \bar{s}_{O_1}$) sides of the body. Curves 1–4 were obtained for the case without injection, and curves 1′–4′ were obtained with allowance for injection of the coolant gas with a flow rate $(\rho v)_w = 1.626$ kg/(m^2·sec). The curves correspond to shells made of copper (curves 1 and 1′), steel (curves 2 and 2′), and coal–plastic (curves 3 and 3′). The radiative equilibrium temperature $T_{w,eq}$ determines the maximum reachable temperature of the surface in the absence of heat overflow in the longitudinal and circumferential directions. On the conical part of the shell, $T_{w,eq}$ is found from the nonlinear relation

$$q_w - \varepsilon\sigma T_{w,eq}^4 = 0,$$

and on the spherical part of the shell, it is found from the condition of conservation of energy on the surface with allowance for the steady solution for a thin porous shell:

$$q_w - \varepsilon\sigma T_{w,eq}^4 = (\rho v)_w c_{p,g}(T_{w,eq} - T_{in}).$$

It follows from Fig. 2 that injection of the coolant gas significantly decreases the steady temperature of the surface and the radiative equilibrium temperature. On the leeward side of the porous spherical bluntness, for example, at the point $\bar{s} \approx -1.35$, the difference in the steady temperature values obtained without and with allowance for injection is approximately 430 K for copper, 750 K for steel, and 1020 K for coal–plastic. The values of the radiative temperature at this point differ approximately by 1050 K.

The clear minimum in the distribution of the radiative equilibrium temperature is caused by displacement of the stagnation point to the windward side, which is due to the motion of the body at incidence. This leads to overflow of an additional mass of the cold coolant gas to the leeward side, which decreases the heat flux and surface temperature. This is manifested in the increase in the parameter b in Eq. (1.16) for the convective heat flux in the screening zone; the parameter b is the ratio of the total mass of the injected gas to the product of the heat-transfer

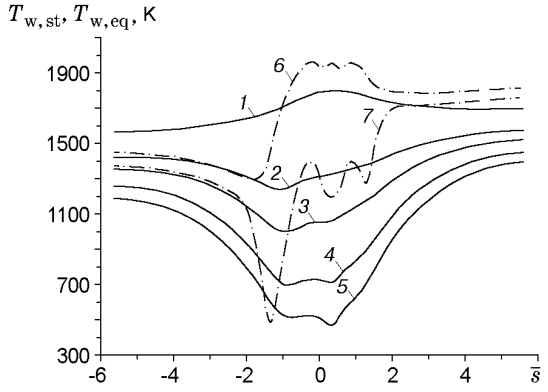

Fig. 3

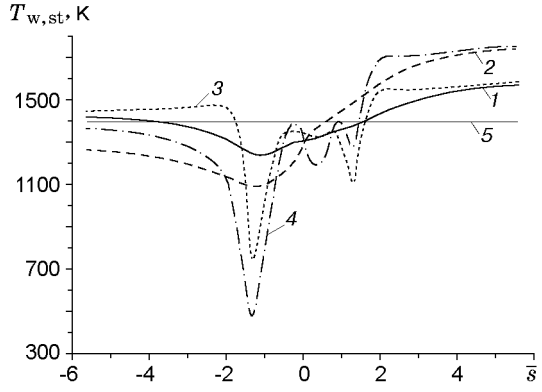

Fig. 4

coefficient in the considered cross section s in the absence of injection and the surface area of the cone from the cross section s_1 to the current value of s [2].

Owing to heat overflow from the peripheral part of the cone to the porous nose, the temperature on the windward peripheral part of the cone decreases with increasing thermal conductivity of the material λ. On the leeward side of the peripheral part of the cone surface, the temperature $T_{w,st}$ changes nonmonotonically, depending on λ. As in the case without injection $(\rho v)_w = 0$ [6], this is caused by the nonmonotonic distribution of the heat flux along the circumferential coordinate η and heat overflow in the circumferential direction. On the porous spherical part, in the vicinity of the frontal critical point, where a laminar boundary-layer flow regime is observed, an increase in the thermal conductivity λ is accompanied by an increase in the steady temperature of the surface.

As it could be expected,the greatest effect of heat overflow is observed for copper, and the smallest effect is observed for coal–plastic. For the latter, the steady temperature of the surface differs insignificantly from the radiative equilibrium temperature, since the heating process is close to one-dimensional. Owing to heat overflow along the longitudinal and circumferential coordinates, the steady temperature of the surface on the peripheral part of the cone on the windward side for copper is approximately 200 K lower than for steel and coal–plastic. On the leeward side, this difference is smaller.

The dependences $T_{w,st}(\bar{s})$ (curves 1–5) and $T_{w,eq}(\bar{s})$ (curves 6 and 7) for various flow rates of injection $(\rho v)_w$ for copper are plotted in Fig. 3 [$(\rho v)_w = 0$ (curves 1 and 6), 1.626 kg/(m$^2 \cdot$ sec) (curves 2 and 7), and 3, 6, and 10 kg/(m$^2 \cdot$ sec) (curves 3, 4, and 5, respectively)]. It follows from Fig. 3 that, as the flow rate of injection increases from 0 to 10 kg/(m$^2 \cdot$ sec), the maximum decrease in the steady temperature of the surface is approximately 1350 K, and the maximum decrease in the radiative equilibrium temperature is 1120 K.

We studied the influence of heat transfer in the directions n_1, $\bar{s}$, and η on the dependence $T_{w,st}(\bar{s})$ for copper, steel, and coal–plastic. For each material considered, the heating problem was solved in one-, two-, and three-dimensional formulations. An analysis of numerical results shows that heat overflow has almost no effect on the distribution of the steady temperature of the surface in the case of coal–plastic and has a small effect in the case of steel, except for the point $\bar{s} \approx -1.35$ where the overflow effect leads to a 100–150 K change in temperature. The effect of heat overflow is rather significant in all directions for copper (Fig. 4). The results in Fig. 4 were calculated for $(\rho v)_w = 1.626$ kg/(m$^2 \cdot$ sec). Curve 1 was obtained with allowance for heat overflow in the directions n_1, $\bar{s}$, and η, curve 2 in the directions n_1 and $\bar{s}$, and cure 3 in the directions n_1 and η. Curve 4 corresponds to the one-dimensional formulation, and curve 5 obtained for $\lambda_i \to \infty$ $(i = 1, 2)$ degenerates into a straight line parallel to the axis $\bar{s}$ due to equalization of the steady temperature profile in the shell. For copper, steel, and coal–plastic, the steady temperature of the surface calculated by the one-dimensional model (variables n_1 and t) coincides in the graph scale with the radiative equilibrium temperature $T_{w,eq}(\bar{s})$, which confirms again the validity of the algorithm and program.

The results of solving the IP for $(\rho v)_w = 1.626$ kg/(m$^2 \cdot$ sec) are plotted in Figs. 5 and 6. Figure 5 shows the distribution of the total heat flux over the contour for $t = 1$ and 5 sec (curves 1 and 2, respectively) for the copper shell (the solid curves are the "exact" solution of the three-dimensional IP constructed on the basis of the DP solution, and the dashed curves are the numerical solution of the three-dimensional IP). Despite the complicated nonmonotonic dependence $Q_w(\bar{s})$ caused by heat overflow and injection, the heat-flux values are determined rather

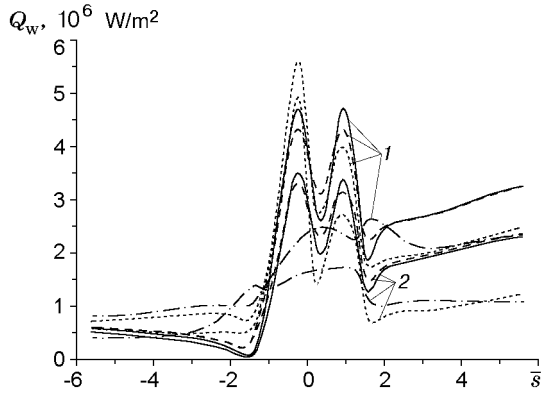

Fig. 5

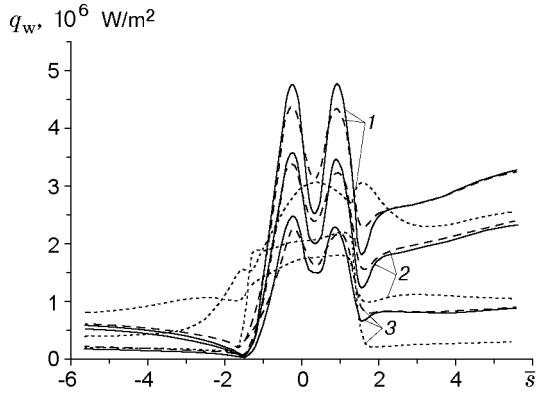

Fig. 6

accurately. At the same time, the neglect of heat overflow along the longitudinal and circumferential coordinates leads to large errors in heat-flux determination. The dot-and-dashed curves show the dependence $Q_w(\bar{s})$ obtained without allowance for heat overflow in the directions $\bar{s}$ and η; the dotted curve shows the results obtained without allowance for heat overflow in the direction η. In all calculation variants, the initial data for the IP were the "exact" solution of the three-dimensional DP for the temperature on the back surface of the shell $T_L^{\exp}(s, \eta, t)$. The results obtained allow us to conclude that it is necessary to use three-dimensional IP algorithms for reconstructing the heat flux to a shell made of a highly heat-conducting material.

Figure 6 shows the results of solving the three-dimensional IP of reconstructing convective heat fluxes on the boundary of highly heat-conducting materials in a wide range of temperatures. The solid curves are the exact solution of the three-dimensional IP for the copper shell, and the dashed curves show the numerical solution with the use of a three-dimensional algorithm. Curves 1–3 correspond to the times $t = 1$, 5, and 200 sec. The results obtained indicate that it is possible to use the developed algorithm of solving the three-dimensional boundary-value IP to interpret the readings of heat-flux gauges if the measurement time is long. The issue of the validity of employing the widely used thin-wall method [13] for determining the heat fluxes on the surface of highly heat-conducting materials with injection was also considered. In this method, the total heat flux on the wall is determined by the following formulas: in the absence of injection,

$$Q_w(\bar{s}, \eta, t) = q_w(\bar{s}, \eta, t) - \varepsilon\sigma T_w^4 = \rho c_p L \frac{dT_w}{dt},$$

and with allowance for injection,

$$Q_w(\bar{s}, \eta, t) = q_w(\bar{s}, \eta, t) - \varepsilon\sigma T_w^4 = \rho c_p L \frac{dT_w}{dt} + (\rho v)_w c_{p,g}(T_w - T_g).$$

The dependence $q_w(\bar{s})$ calculated by the thin-wall method is plotted in Fig. 6 by the dotted curves. The results obtained indicate that it is not reasonable to use this method for reconstructing heat fluxes in the case highly heat-conducting materials.

As in [6], the effect of the errors of definition of the initial temperature $T_L^{\exp}(s, \eta, t)$ on the IP solution was studied. For this purpose, temperature perturbations in time were prescribed according to a saw-tooth law; the amplitude of perturbations was 1% of the current temperature values at points with the coordinates $\bar{s} = 0.89$ and 1.04. Smoothing of the perturbed temperature by Tikhonov's regularization method allowed us to obtain a steady solution of the three-dimensional IP, which was in good agreement with the exact solution.

Thus, the influence of heat overflow along the longitudinal and circumferential coordinates and the effect of injection of a coolant gas on the characteristics of spatial heat transfer were considered using the developed algorithms of solving three-dimensional direct and inverse heat-transfer problems. The joint use of highly heat-conducting materials and injection of a coolant gas was shown to be efficient for decreasing the maximum temperatures on heat-loaded sectors of the shell of the wetted body. The error of using one- and two-dimensional algorithms of solving DP and IP and the thin-wall method in reconstructing heat fluxes on the surface of highly heat-conducting materials was estimated.

This work was supported by the Russian Foundation for Fundamental Research (Grant No. 99-01-00352).

REFERENCES

1. V. I. Zinchenko, A. G. Kataev, and A. S. Yakimov, "Investigation of the temperature regimes of bodies immersed in flow with surface blowing," *J. Appl. Mech. Tech. Phys.*, **33**, No. 6, 821–827 (1992).
2. V. I. Zinchenko, V. I. Laeva, and T. S. Sandrykina, "Calculation of temperature regimes for streamlined bodies with various thermal properties," *J. Appl. Mech. Tech. Phys.*, **37**, No. 5, 703–709 (1996).
3. V. I. Zinchenko and A. S. Yakimov, "Heat-transfer characteristics in flow around a spherically blunted cone at incidence and gas injection from a blunted surface," *J. Appl. Mech. Tech. Phys.*, **40**, No. 4, 697–703 (1999).
4. V. I. Zinchenko and A. Ya. Kuzin, "A study of heat-transfer processes in a supersonic flow around a spherically blunted cone with allowance for injection of a gas–cooler," *J. Appl. Mech. Tech. Phys.*, **40**, No. 5, 886–894 (1999).
5. V. I. Zinchenko and A. Ya. Kuzin, "Study of the thermal state of a spherically blunted cone in a hypersonic spatial flow by methods of solving direct and inverse problems of heat and mass transfer," in: *Proc. IV Int. Forum on Heat and Mass Transfer* (Minsk, May 22–26, 2000), Vol. 3, Lykov Heat and Mass Transfer Institute, Belarus National Acad. of Sci. (2000), pp. 83–90.
6. V. I. Zinchenko and A. Ya. Kuzin, "Effect of heat overflow on heat-transfer characteristics in a supersonic spatial flow around a spherically blunted cone," *J. Appl. Mech. Tech. Phys.*, **43**, No. 1, 144–152 (2002).
7. O. M. Alifanov, "Inverse problems as the methodological basis for identification of thermal mathematical models," in: *Proc. IV Int. Forum on Heat and Mass Transfer* (Minsk, May 22–26, 2000), Vol. 3, Lykov Heat and Mass Transfer Institute, Belarus National Acad. of Sci. (2000), pp. 3–13.
8. O. M. Alifanov, *Identification of Heat-Transfer Processes on Flying Vehicles* [in Russian], Mashinostroenie, Moscow (1979).
9. O. M. Alifanov and A. V. Nenarokomov, "Three-dimensional inverse problem of heat conduction in an extreme formulation," *Dokl. Akad. Nauk SSSR*, **325**, No. 5, 950–954 (1992).
10. O. M. Alifanov and A. V. Nenarokomov, "Three-dimensional boundary-value inverse problem of heat conduction," *Teplofiz. Vys. Temp.*, **37**, No. 2, 231–238 (1999).
11. A. Ya. Kuzin, "Identification of heat- and mass-transfer processes in reacting media," in: *Conjugate Problems of Mechanics and Ecology* (collected scientific papers) [in Russian], Izd. Tomsk. Univ., Tomsk (2000), pp. 190–205.
12. B. A. Zemlyanskii and G. N. Stepanov, "Calculation of heat transfer in a spatial flow around thin blunted cones by a hypersonic air flow," *Izv. Akad. Nauk SSSR, Mekh. Zhidk. Gaza*, No. 5, 173–177 (1981).
13. Yu. V. Polezhaev and F. B. Yurevich, *Thermal Protection* [in Russian], Énergiya, Moscow (1976).
14. V. N. Kharchenko, "Heat transfer in a hypersonic turbulent boundary layer with injection of a coolant gas through a slot," *Teplofiz. Vys. Temp.*, No. 1, 101–105 (1972).
15. V. I. Zinchenko and O. P. Fedorova, "Study of a three-dimensional turbulent boundary layer with allowance for coupled heat transfer," *J. Appl. Mech. Tech. Phys.*, **30**, No. 3, 451–457 (1989).
16. A. V. Bureev and V. I. Zinchenko, "Calculation of a spatial flow around spherically blunted cones in a vicinity of the plane of symmetry with different flow regimes in the shock layer and gas injection from the surface," *Prikl. Mekh. Tekh. Fiz.*, No. 6, 72–78 (1991).
17. N. N. Yanenko, *Method of Fractional Steps in Solving Multidimensional Problems of Mathematical Physics* [in Russian], Nauka, Novosibirsk (1967).
18. A. M. Grishin, A. Ya. Kuzin, V. L. Mikov, et al., *Solution of Some Inverse Problems of Mechanics of Reacting Media* [in Russian], Izd. Tomsk. Univ., Tomsk (1987).
19. A. A. Samarskii and E. S. Nikolaev, *Methods for Solving Grid Equations* [in Russian], Nauka, Moscow (1978).
20. A. M. Grishin and V. N. Bertsun, "Iterative–interpolation method and spline theory," *Dokl. Akad. Nauk SSSR*, **214**, No. 4, 751–754 (1974).
21. C. H. Reinsch, "Smoothing by spline functions," *Numer. Math.*, **10**, 177–183 (1967).
22. O. M. Alifanov, V. K. Zantsev, B. M. Pankratov, et al., *Algorithms of Diagnostics of Heat Loads of Flying Vehicles* [in Russian], Mashinostroenie, Moscow (1983).
23. Yu. S. Zav'yalov, B. I. Kvasov, and V. L. Miroshnichenko, *Methods of Spline Functions* [in Russian], Nauka, Moscow (1980).
24. A. Ya. Kuzin and N. A. Yaroslavtsev, "Application of regularization algorithms for solving a nonlinear boundary-value inverse problem of heat conduction," Tomsk Univ. (1987). Deposited at VINITI 07.22.87, No. 5280 V87.
25. V. A. Antonov, V. D. Gol'din, and F. M. Pakhomov, *Aerodynamics of Bodies with Injection* [in Russian], Izd. Tomsk. Univ., Tomsk (1990).